Five simple tools for stochastic lattice creation

Jan-Hendrik Groth[a,c], Caelan Anderson[a], Mirco Magnini[b], Christopher Tuck[c], Adam Clare[a,*]

[a]*Advanced Manufacturing Group, Faculty of Engineering, The University of Nottingham, NG7 2RD Nottingham, U.K.*
[b]*Fluids and Thermal Engineering Research Group, Faculty of Engineering, The University of Nottingham, Nottingham, NG7 2RD, U.K.*
[c]*Centre for Additive Manufacturing, Faculty of Engineering, The University of Nottingham, Nottingham, NG7 2RD, U.K.*

Abstract

Lattices are increasingly used in engineering applications. They can reduce weight in aircraft components, increase the efficiency of heat exchangers and are used as medical implants. Typically a regular and graded lattice, where the unit cells are iterated one after another is used. Although methods exist to create stochastic lattices, they are limited to apply only one randomness to all lattice defining parameters (isotropic randomness). However, nature suggests a different value of randomness for each parameter (anisotropic randomness). Here we demonstrate five new approaches to create a stochastic lattice to enable novel structure creation. Firstly, a tool to create isotropic randomness, secondly, a way to create anisotropic randomness, thirdly, an approach to create graded randomness, fourthly, a feature to create layered randomness controlled by a function, and finally, we create a lattice with stochastic surface roughness. These techniques will provide new possibilities in designing true biomimetic medical implants, heat exchangers and mechanical components.

Keywords: stochastic lattice, cellular material, stochastic grading, additive manufacturing

*Corresponding author. Tel.: (+44) 115 951 4109.
Email address: adam.clare@nottingham.ac.uk (Adam Clare)

1. Introduction

A cellular material is a structure formed by a system of vertices joined by struts or surfaces [1]. It can be classified into random structures, so called foams or stochastic lattices as well as into architectured materials which are called lattices [2].

Traditionally, foams may be produced by a number of manufacturing processes [3]. Amongst other processes, a foaming agent can be used in the melt or mixed with powder to start a foaming process that yields to many cavities within the material, which form a foam. Also, gas can be introduced to follow the same route. However, these processes are restricted to specific materials and the band of achievable cell sizes and relative densities highly depend on the method of manufacture [3].

Moreover, wires were also used and arranged to resemble a lattice [4] to investigate the heat transfer capabilities. However, from the way these wires are designed, it can be assumed that these are not easy to integrate into many engineering designs.

Alternatively, foams and lattices can be produced by additive manufacturing, which gives more design freedom. They are included in many commercially available software to create infill structures, and they are used in many engineering applications that are required to be lightweight [5]. A review by Benedetti et al. [2] shows many different types of cellular materials in use: the strut based lattices and the triply periodic minimal surfaces (TPMS) that form networks or sheets. This review focuses on the fatigue properties of different lattices manufactured by additive manufacturing. Al-Ketan et al. [6] presented a review that focuses on TPMS structures and shows, amongst others, the mechanical properties that were investigated and the applications for which TPMS structures were used. In these reviews, stochastic lattices played only a marginal role but are worthy of further exploration. The methods to design stochastic lattices with varying degrees of randomness can be traced back to several papers.

Three methods exist to create controllable stochastic lattices. By controlled stochasticity or controlled randomness, we mean that any pseudo-random distribution creates numbers within a defined control space (2D) or volume (3D). For brevity, we continue to use random instead of pseudo-random.

The method used by van der Burg et al. [7] starts with a periodic pattern composed of points. Here this is defined as the first method. Each point has coordinates x_n, y_n (2D) and z_n (3D) in a given design space. Where n represents the point number. An individual step distance Δx_n, Δy_n, Δz_n, generated by a uniform random dis-

tribution is added to each coordinate. By controlling the allowable step distance, they were able to define the control volume of each point. This gives $x_n + \Delta x_n$, $y_n + \Delta y_n$, and $z_n + \Delta y_n$, and the points are randomised. The periodic pattern was created from different unit cells (UC). The UCs used were body centred cubic (BCC), face centred cubic (FCC) and hexagonal close-packed (HCP). These randomly distributed points were then used as seeding points for a Voronoi algorithm to create struts of uniform thickness. The randomness was measured as the step length of the uniform distribution divided by the UC length. Van der Burg et al. [7] showed that by increasing the randomness of the basic UC, the Poisson's ratio and the Young's modulus increase. The first method was also used by Roberts et al. [8]. They periodically placed spheres in a design space. Then the displacement of each sphere was determined by a Monte-Carlo method. They controlled these spheres such that they did not overlap. However, the randomisation was not controlled. They also applied another method by creating a Gaussian Random Field from which they generated a lattice structure by evaluating the threshold value of an isosurface. Moreover, they connected randomly distributed points by using a nearest neighbour node-bond model. Methods like the Gaussian Random field, where random nodes are created without a set of rules, is here considered as the second method.

Luxner et al. [9] applied a method using a spatial random distribution and controlled the random distribution by a step distance. The periodic array was populated with different UCs. The used UCs are a simple cubic, a Gibson-Ashby, a reinforced BCC, a BCC, a Kelvin, and a Weaire Phelan lattice. The vertices of the lattices were connected by struts using a feature included in Abaqus. A Finite Element Analysis (FEA) of the simple cubic and Kelvin structure showed that the simple cubic structure had the highest elastic modulus anisotropy in the [001] direction. In contrast, the Kelvin structure could be considered isotropic. The increase of randomisation showed a decrease of the elastic modulus in the [001] direction leading to a lower anisotropy. However, the elastic modulus of the Kelvin structure was reduced in all directions with increasing randomness. Comparing this to van der Burg et al.'s [7] structures, the elastic modulus did not increase. This implies that the influence on the elastic properties depends on the used UC and randomness. Yang et al. [10] proposed a method, which could be categorised as method one, too. The UC is a Schwarz Primitive TPMS structure, described by an implicit function $\phi(x, y, z)$. Here, the parameters x, y, z are altered by a random distribution function similar to a Gaussian distribution. This randomises every coordinate directly. The result is a stochastic TPMS lattice.

Another method used by Silva et al. [11] created random 2D Honeycomb struc-

tures using a uniform distribution from which random values are generated for the node coordinates. Then they populate node after node into a design space. While populating each node, every subsequent node's distance to the previous was checked to be in a controlled volume. This method is the third method. An FEA showed that the difference between the elastic properties of 2D Honeycombs with randomness and without randomness is statistically insignificant. The third method was also used in four publications by Zhu et al. for 3D [12], [13], 2D randomised Honeycombs [14], and in the explanation of the method [15]. All four studies create a starting point from which they introduce more points with coordinates generated by a random uniform distribution. A minimum step distance controlled the randomness. Firstly, Zhu et al. [14] investigated 2D Voronoi Honeycombs' mechanical properties using an FEA approach. They showed that the Young's Modulus and Shear Modulus increase with increasing randomness. On the contrary, the Bulk Modulus showed a lower value at increasing randomness. Interestingly, the higher Young's modulus was observed for relative densities lower than 0.2. At values higher than 0.2, it seems that the Young's modulus of the fully random Voronoi Lattice is lower than the regular Voronoi Lattice. At low relative densities smaller than 0.05, Zhu et al. [14] show that the Poisson's ratio is similar for the randomised lattices and the regular lattice. However, with increasing relative density, the Poisson's ratio of the fully random lattice is lower than the regular lattice's Poisson's ratio. In [12], Zhu et al. compared a regular tetrakaidecahedron 3D Voronoi lattice with a randomised 3D Voronoi Lattice. They show that the randomised lattices have a higher Young's modulus and shear modulus than the regular lattice. Moreover, the Bulk modulus is decreasing with increasing randomness. Additionally, Zhu et al. [13] also studied the influence of the randomisation of 3D Voronoi lattices on the stress and strain behaviour. They showed that the randomised lattices are stiffer than the regular lattice up to a strain of roughly 0.2 to 0.3. After a strain of 0.2 and 0.3, the random lattice's stress flattens and forms a plateau, while the stress of the regular lattice is still increasing. However, the relative density was 0.01. This gives rise to the question of how these lattices would behave when additive manufactured. Because the relative densities in Zhu et al. studies are in general relatively low. The second method was also applied in two publications by Martínez et al. In their earliest publication, Martínez et al. [16] used a Poisson disc sampling approach to allocate seeding points for a subsequent Voronoi Tesselation. By varying the number of seed points within certain regions of a design, they can tailor the elasticity to create compliant designs, additively manufacture them and investigate their elastic properties. Using the same seed point generation and stretching the Voronoi cells

according to stress fields, Martínez et al. [17] created orthotropic elastic properties. These were applied to a gear and a chair. However, they were not able to create anisotropic designs. McConaha et al. [18] solved this by relying on randomly distributed points that the Llyod Algorithm rearranged to create centroidal Voronoi diagrams in 2D. By stretching the created cells according to anisotropy fields, they were able to create anisotropic Voronoi cells. Even though Martínez et al. and McConaha et al. rely on random seed points, they are not tailoring the randomness.
Another method that does not fit the proposed randomisation categories was used by Mirzaali et al. [19]. They used a honeycomb structure with two different UC strut angles and mixed them randomly to create an auxetic structure. By controlling the proportions of UC a with an angle α and a UC b with with an angle β, they used a random uniform distribution and divided the set of numbers into two parts with changing probability. In that way, they were able to control the Poisson's ratio of an auxetic lattice. A more recent study by Mueller et al. [20] compared the energy absorption of regular lattices with different connectivity and different rotation angles with random lattices with the same connectivity. They showed that random lattices are advantageous in energy absorption applications due to the ability of random lattices to absorb energy more evenly. The regular lattices showed many stress peaks before compacting what the random lattices did not show. In Mueller et al. [20], the random lattices were created by method one, where a random continuous uniform distribution was created for the coordinate of each point to randomise it. These lattices were not additively manufactured. However, random Voronoi lattices were recently additively manufactured and investigated by Maliaris et al. [21]. Their impact properties were studied through impact experiments and an FEA analysis. The analysis showed good energy absorption behaviour of these random lattices which makes them candidates for many energy absorption applications. Moreover, currently free available tools like MSLattice [22] and FLatt Pack [23] offer a variety of lattices and functionality. Still, they do not offer the functionality to create stochastic lattices.Commercial software like nTopology [24], [25] and Autodesk Within Medical [26] offer the use of creating stochastic lattices and the creation of rough surfaces. However, the methodology is not available which is a limit for academic usage. In contrast to adding surface roughness computationally, ways were explored in additive manufacturing. Hence, the surface roughness was manipulated using machine parameters [27] as well as exploiting the staircase effect [28].

It is worthy of mention that the use of cellular materials in mechanical designs

is linked to Biomimicry in du Plessis's review on the subject [29]. Biological designs like shark denticles teach us that randomness in nature must be different for different parameters such as length, width, skew or roughness [30].By evaluating the dimensional distribution, the standard deviation σ divided by the corresponding average parameter, relative randomness values can be calculated. Typically, the relative randomness can vary between 2-9 % for the length, 5-42 % for the roughness, 1-8 % for the aspect ratio (length divided by width), and 6-48 % for the skew of shark denticles for one species [30]. The beech tree, by way of another example, also shows different levels of randomness across parameters: the tree height's and specific leaf size's relative randomness ranges from 1-4 %, and the tree's trunk diameter relative randomness at 'human breast height' varies from 5-11 % [31]. If these parameters are considered design input parameters, it is evident that randomness must be tailored. Hence, let us consider a regular distribution of points in a 2D system where each point's x and y coordinate can be regarded as a controllable parameter. To apply randomness to a regular array fig. 1 a), two simple cases exist. The same randomness can be applied to the x and y parameter fig. 1 b), which we call isotropic randomness, or x and y have a different randomness parameter fig. 1 c). This is anisotropic randomness. It can be seen that for a randomisation $\sigma_x < \sigma_y$, the dots appear to be more aligned in the y-direction. is important to notice that the introduced terms isotropic and anisotropic randomness should not be confused with isotropic or anisotropic material properties.

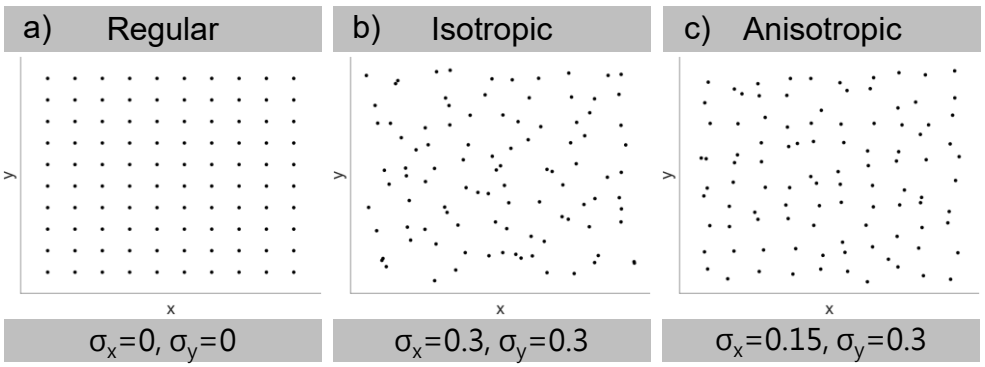

Figure 1: a) shows a regular arrangement of points. b) illustrates isotropic randomness superimposed on the regular array a). c) is demonstrating anisotropic randomness added to the regular array a).

The reported literature that creates stochastic lattices shows significant lim-

itations. Firstly, the same randomisation for all parameters is used, which we previously defined as isotropic randomness. Secondly, the randomisation cannot be graded within the lattice. Thirdly, the struts are subject to a uniform thickness. Fourthly, locations with higher stochasticity cannot be created. Fifthly, roughness cannot be added to the lattice surface, which would benefit thermo-mechanical applications. Here we present a novel toolset to create stochastic lattices that overcomes these limitations. Firstly, we introduce the different UCs which create the regular distribution of points. On these points, we will position ellipsoids. A Gaussian distribution is then used to create the different randomisation offsets for each ellipsoid's parameters. We can solve the first problem by using different randomisation values for the various ellipsoid's parameters, leading to anisotropic randomness. By using a linear gradient, we can increase the randomness in different directions. This solves the second limitation. Using ellipsoids, where we can manipulate the radius in different directions, we can achieve non-uniform strut thicknesses. By creating a stochastic sine layer inside the lattice, we can create a layer of randomness which solves the fourth limitation. Moreover, by randomly varying the surface, we can create roughness and overcome the fifth limitation. Hence, we demonstrate five simple tools which include isotropic randomness, anisotropic randomness, graded randomness, layered randomness, and surface roughness. These features can be used for thermo-mechanical, energy absorption or frequency dampening. Moreover, it gives researchers a tool to perform necessary experiments to investigate the mechanical properties.

2. Methodology

Here we describe the methodology to design a stochastic lattice. The methodology was implemented in MATLAB R2020b. The general program flow can be seen in fig. 2. Firstly, a desired 'parent' lattice UC is selected, for example, a cubic UC. All lattice types are compatible with this methodology to the knowledge of the authors. Afterwards, the UC parameters are defined. These are the cell size u_x, u_y and u_z, the lattice volume dimensions l_x, l_y and l_z, and the relative density RD. Again this parameter set can be greatly expanded to describe any lattice type or geometry. Then the randomisation process is defined: isotropic randomness, anisotropic randomness, graded randomness, layered randomness. Stochastic roughness can be applied after the lattice creation, which may result in change of the RD. For each randomness prescription, specific parameters are defined. After the randomisation process, 0esulting binary matrix is smoothed by using MATLAB's smooth function and the relative density is adjusted within

±0.01 to achieve the desired relative density. If roughness is applied, smoothing is not applied. Subsequently, the faces and vertices of the lattice are determined via MATLAB's isosurface and isocaps function. Then the faces and vertices were exported to an STL file by the available function 'stlwrite' [32]. The 'stl' files were then visualised by using AutoDesk Meshmixer.

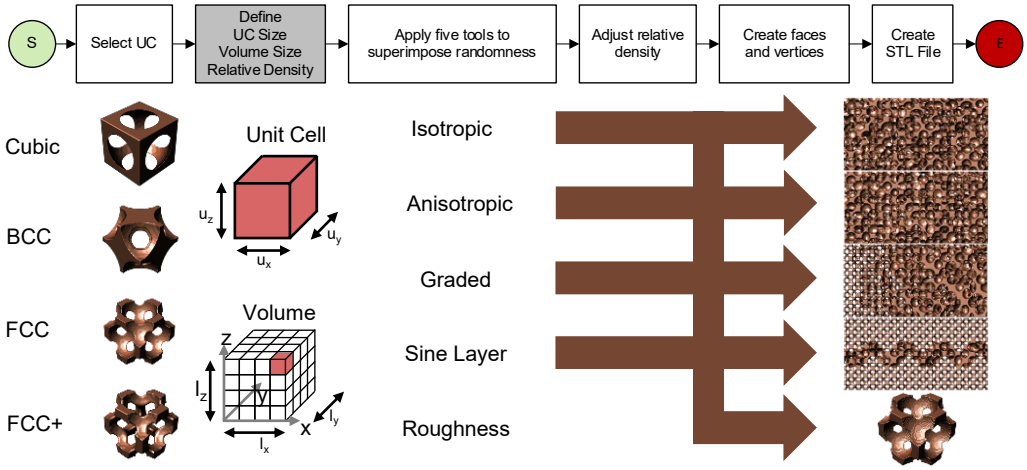

Figure 2: The stochastic lattice script program flow. A UC is selected, and its dimensions are defined. Then the lattice control volume is defined, and the desired relative density is set. Then five tools can be applied to the defined volume: isotropic randomness, anisotropic randomness, graded randomness, layered randomness. The stochastic roughness can be applied to each randomisation tool after the RD adjustment. After that, the relative density is adjusted to reach the desired relative density. Finally, the lattice's vertices and faces are created and saved as an STL file.

2.1. Regular Lattice

Let us consider a UC in the shape of a cube, fig. 3 a). The length of each side can be described by u_x, u_y and u_z.

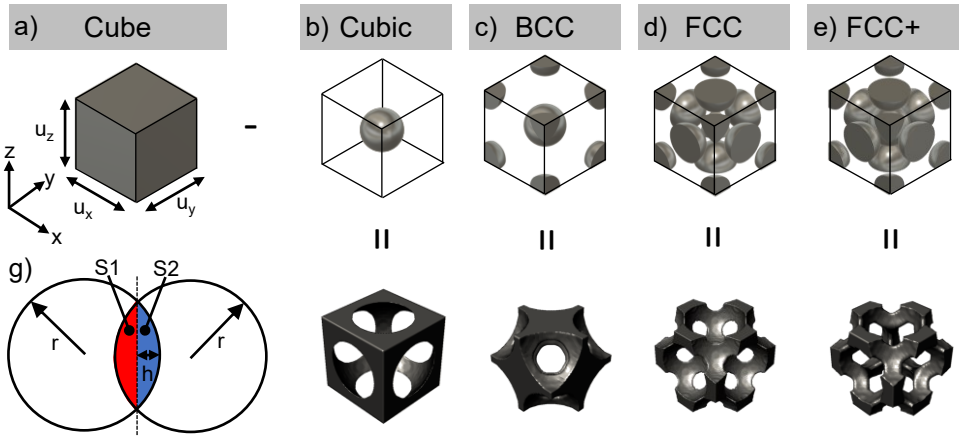

Figure 3: a) shows a basic cube UC defined by u_x, u_y and u_z. By subtracting the UCs b)-e) from a), a Cubic, BCC, FCC and FCC+ UC is created. g) shows the case of two overlapping circles where two segments $S1$ and $S2$ appear.

A UC is the initial regular structure that is periodically distributed within the design space. Here we populate a cubic, a BCC, an FCC, and an FCC+ UC. The FCC+ UC is the union of the cubic and FCC UC. The UCs are shown in fig. 3 b) - e). On each of the nodes, which are represented by 1/8th, a half, or a full sphere in fig. 3, a sphere is placed. The sphere can be calculated by the implicit function of an ellipsoid (1).

$$\phi(xc_n, yc_n, zc_n, rx_n, ry_n, rz_n) = \frac{xc_n^2}{rx_n^2} + \frac{yc_n^2}{ry_n^2} + \frac{zc_n^2}{rz_n^2} \tag{1}$$

An ellipsoid was chosen to create a sphere to control several parameters after applying the randomisation. In that way, the sphere can be stretched in many directions. Here, xc_n, yc_n, zc_n describe the n-th ellipsoid's centre position, while rx_n, ry_n, and rz_n describe the n-th ellipsoid's radius in the x, y, and z-direction. The applied relative density RD defines the final lattice volume $V_{Lattice}$ eq. (2).

$$V_{Lattice} = RD \cdot V_{cube} \tag{2}$$

The cube's volume V_{cube} is defined by eq. (3), if, as in this case, $u_x = u_y = u_z$.

$$V_{cube} = u_x^3 \tag{3}$$

To determine the sphere's radius, the following equations are solved for two special cases, eq. (4). Case 1: $RD \geq RD_{Limit}$ is the closed-cell structure, and Case 2:

is the open-cell structure $RD < RD_{Limit}$. p is the number of spheres within one UC, and q is the number of overlapping segments. RD_{Limit} is the point where the UC transitions from closed cells to open cells.

$$V_{Lattice} = \begin{cases} V_{Cube} - p \cdot V_{Sphere} & RD \geq RD_{Limit} \\ V_{Cube} - p \cdot V_{Sphere} + q \cdot V_{Segment} & RD < RD_{Limit} \end{cases} \tag{4}$$

The UC parameters p, q, and RD_{Limit} are described in tab. 1. The sphere in eq. (4)

Table 1: The parameters to determine the radius of a Cubic, BCC, FCC, and FCC+ UC. p is the number of full spheres within a UC, q is the total number of overlaps and RD_{Limit} is the limit where the UC shifts from a closed-cell to an open-cell.

Unit Cell	p	q	RD_{Limit}
Cubic	1	6	$1 - \frac{1 \cdot \pi}{6}$
BCC	2	16	$1 - \frac{\sqrt{2} \cdot \pi}{8}$
FCC	4	48	$1 - \frac{\sqrt{2} \cdot \pi}{6}$
FCC+	5	12	$1 - \frac{5 \cdot \pi}{48}$

can be described by eq. (5).

$$V_{Sphere} = \frac{4 \cdot \pi}{3} \cdot r^3 \tag{5}$$

Each segment's volume $V_{Segment}$ can be calculated by eq. (6) due to overlapping spheres, where h is the height of one segment, as shown in fig. 2 g).

$$V_{Segment} = \frac{\pi}{3} \cdot (r - h)^2 \cdot (2 \cdot r + h) \tag{6}$$

2.2. Parameter Randomisation

To randomise the lattice structure, it is necessary to superimpose a random distribution to all of the parameters describing the ellipsoid eq. (1). This gives a total of six parameters that can be subject to randomisation. For simplicity, we will explain the randomisation process for xc_n (the method is identical for all other parameters). The randomisation is introduced by moving xc_n by a certain random distance Δxc_n, eq. (7), which gives a randomised value $xcran_n$.

$$xcran_n = xc_n + \Delta xc_n \tag{7}$$

The random distance Δxc_n is created by a Gaussian distribution, eq. (8).

$$f(\Delta xc_n|\mu,\sigma) = \frac{1}{\sqrt{2\pi}\cdot\sigma}\cdot e^{-0.5\cdot(\frac{\Delta xc_n-\mu}{\sigma})^2} \tag{8}$$

A mean value μ describes the Gaussian distribution. In this work, if not otherwise specified, μ is assigned to be zero because the parameters of the regular UC was already defined. The standard deviation σ is the control parameter (or randomisation value), used to control the location where the random values are created around μ. For a Gaussian distribution, roughly 68 %, 95 %, and 99% of randomly distributed values are created within σ, 2σ, and 3σ, respectively. This allows isotropic and anisotropic randomness to be described geometrically (see fig. 1).

2.3. Graded Randomness

Another way to exploit randomness is to grade randomness. Lattice parameters like the cell size, strut thickness or wall thickness have been graded previously [22]. However, any parameter including randomness can be graded by the same principle. Here we grade the standard deviation σ of the Gaussian random distribution eq. (8) by a linear function eq. (9) in the x-direction. It is the same for the y and z-direction. Consider position x=0 with a randomisation of $\sigma_{x=0}$, and $x = l_x$ with a randomisation of $\sigma_{x=l_x}$. Then a linear gradient increases the randomness from position 0 to position l_x from, for example, $\sigma = 0$ to $\sigma = 0.3$.

$$\sigma(x) = \frac{\sigma_{x=l_x} - \sigma_{x=0}}{l_x}\cdot x + \sigma_{x=0} \tag{9}$$

2.4. Randomised Layers

When randomising lattice structures, it is also possible to design sandwich structures, where a randomised lattice layer (red) is enclosed within two regular lattice layers (white), see fig. 4 a). Here the layer is demonstrated by a 2D section in the x-z plane with a length of l_x and l_z. A height h describes this layer within the lattice volume. This height h describes the position within the volume and depends on the length of the volume in z-direction l_z and divider d. d determines at which position the layer can be found. The layer has a thickness, which can be described by t.

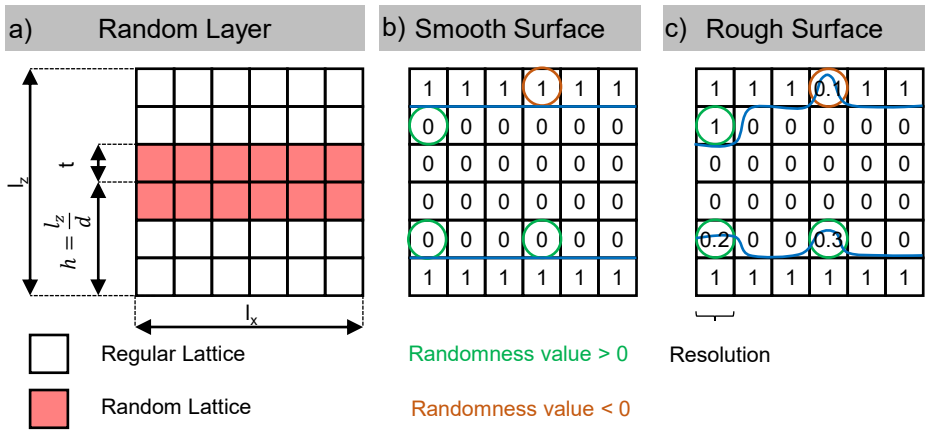

Figure 4: a) Random Layer of thickness t at a height h and overall lattice dimensions of l_x and l_z in the x-z-plane. b) A smooth surface represented by an isosurface blue at a threshold value of zero. The isosurface separates the solid material (1) from the void (0). Values close to the surface are selected according to a randomness value. For randomness values > 0, every third zero surface value is selected, and for randomness values < 0, every third one surface value is selected. c) The rough surface was created by adding the roughness values to the selected surface values. This alters the isosurface (blue) and hence creates roughness.

To describe this flat layer, we chose a sine function to demonstrate versatility. In the future, this could help to tailor this layer to address fluid or vibration problems. Let us assume that all ellipsoids have been created and form a volume with a regular lattice structure. Each ellipsoid's radii $rx_{i,j,k}$, $ry_{i,j,k}$, $rz_{i,j,k}$, and centre positions $xc_{i,j,k}$, $yc_{i,j,k}$, $zc_{i,j,k}$ can be described. i, j, k stand for the matrix coordinates, where the parameters of each ellipsoid are stored. The parameters are stored in an ordered sequence, so that $i = j = k = 1$ is the first ellipsoid close to the lattice's coordinate system. Moreover, $i = j = k = n$ is then the last ellipsoid. Hence, i,j,k correlate with the coordinate system x, y, z. To find the suitable i, j, k values for $zc_{i,j,k}$ to achieve a sine layer, the value k has to be expressed by a sine function that propagates along the x-direction, which is i. Then k can be described by eq. (10). In eq. (10), a is the amplitude, pd is the periodicity, and h is the predetermined height.

$$k(i) = round(a \cdot sin(pd \cdot i) + h) \tag{10}$$

The randomisation of the ellipsoid's centre coordinates and radii can be described by eq. (11). Here $zc_{i,j,k}$ is used in this example but the procedure is the same for the other coordinates and radii. The randomised centre coordinate $zcran_{i,j,k}$ is the sum of the centre coordinate $zc_{i,j,k}$ and the random value $\Delta z_{i,j,k}$ which originates

from eq. (8)).

$$zcran_{i,j,k} = zc_{i,j,k} + \Delta z_{i,j,k} \tag{11}$$

The thickness of the layer at k is just one layer of points. Thickness can be created by setting the point layer within the matrix between $-t$ to t. Then the layer can be described by eq. (12).

$$-t < i < t \tag{12}$$

2.5. Creating surface roughness

Every lattice created after the randomisation process can be described by a binary matrix. In the binary matrix, zero represents a void and one stands for the solid. If MATLAB's iso-surface function is used at a threshold value of zero, the computed faces and vertices describe a surface just at the boundary between the solid (1) and the void (0). The surface is represented by a blue line in fig. 4. To apply the surface roughness, the binary matrix needs to be altered before applying the iso-surface function. This can be done by finding the transition from 0 to 1 or 1 to 0 in the control volume $V_{i,j,k}$. Then the Gaussian random distribution eq. (8) is used to create positive and negative values of $\Delta rough$ around the mean value μ_{rough} by controlling σ_{rough}. The negative values are then added to 1 and the positive values to 0, see eq. (13). If the roughness value is zero, no roughness is added.

$$V_{i,j,k} = \begin{cases} 1 + \Delta rough & if\ \Delta rough < 0 \\ 0 + \Delta rough & if\ \Delta rough > 0 \end{cases} \tag{13}$$

This will result in a rough surface fig. 4 b). Here we manipulate every third value. This results in an isosurface (blue) with irregularities/ roughness. The roughness depends on the selected resolution. Hence, the roughness will vary between two matrice's entries. Subsequently, the iso-surface function can be applied and the faces and vertices can be computed.

2.6. Lattice Parameters

Table 2 shows the lattice parameters that were used to design the lattices in the following section.

Table 2: The lattice parameters used to construct the lattice geometries in this publication. The parameter $U_{x,y,z}$ is the UC size. $l_{x,y,z}$ the expansion of the lattice in the x, y and z-direction. *RD* is the relative density, *MR* is the mesh resolution and d, t, p are the divider, thickness and periodicity that define the sine function. The values for the small, ring, middle and index finger, and thumb are shown.

Function	$U_{x,y,z}$	$l_x/l_y/l_z(mm)$	*RD*	*MR*	*d*	*t*	*p*
Isotropic	5 mm	25/25/25	0.2	0.2 mm	-	-	-
Anisotropic	5 mm	25/25/25	0.2	0.2 mm	-	-	-
Grading	5 mm	50/25/25	0.2	0.2 mm	-	-	-
Sine 0	5 mm	25/25/25	0.2	0.2 mm	2	4	1
Sine I	5 mm	25/25/25	0.2	0.2 mm	2	4	0.25
Sine II	5 mm	25/25/25	0.2	0.2 mm	2	4	0.5
Roughness	10 mm	60/30/30	0.2	0.2 mm	-	-	-
Small	5 mm	Boolean	0.1	0.2 mm	-	-	-
Ring	10 mm	Boolean	0.2	0.2 mm	-	-	-
Middle	10 mm	Boolean	0.2	0.2 mm	-	-	-
Index	5 mm	Boolean	0.2	0.2 mm	2	4	0.5
Thumb	15 mm	Boolean	0.2	0.2 mm	-	-	-

2.7. Additive Manufacturing

The stochastic lattices were manufacturing through selective laser sintering (SLS) on an EOS EOSINT P100 Formiga. The process parameters used in this research group [33] are displayed in tab. 3. After manufacturing, excess Nylon 12 powder was removed from the stochastic lattices. Then the stochastic lattices were sandblasted, followed by a clean-up with pressurised water. After that, the stochastic lattices were cleaned in an ultrasonic bath and then dried in an oven.

Table 3: EOS EOSINT P100 Formiga SLS Nylon 12 process parameters [33].

Material	Laser Power	Layer Thickness	Scan Speed	Hatch Spacing	Chamber Temperature
Nylon 12	21 W	100 μm	2500 mm/s	250 μm	173 °C

3. Results

3.1. Function I: Isotropic Randomness

Figure 5 demonstrates the isotropic randomness applied to lattices composed of Cubic, BCC, FCC+ and FCC UCs, demonstrating the versatility of this approach. A randomness of $\sigma = 0$, $\sigma = 0.15$, and $\sigma = 0.3$ was applied to each lattice. At $\sigma = 0$ all lattices are regular. By increasing the randomness to $\sigma = 0.15$, and $\sigma = 0.3$, it can be seen how the randomness increases. The FCC lattice structure was also manufactured through SLS.

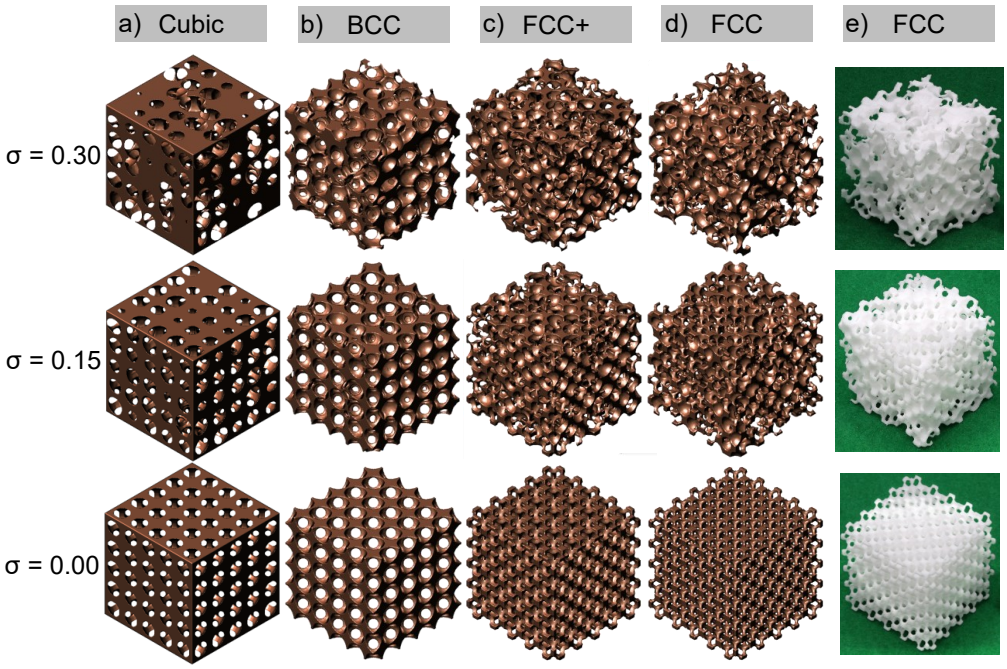

Figure 5: Isotropic randomness applied to a Cubic a), BCC b), FCC+ c) and FCC d) UC. e), the FCC UC is presented as manufactured by SLS. The randomness σ ranges from 0.00 over 0.15 to 0.3 mm.

To confirm that the tools produce the desired randomisation, the randomised coordinates and raddii of the isotropic FCC lattice was evaluated as shown in fig. 6. a) - f) show histrograms with a symmetric distribution. The deviation from the input randomisation 0.15 is small and the variation is within expected ranges. The lowest randomisation value was found at $\sigma_{rx} = 0.136$ and the highest value

was observed at $\sigma_y = 0.149$. An evaluation of the RD of the FCC isotropic lattice at a randomisation of 0.15 showed that the RD of the lattice was 0.213 compared to the 0.21 desired RD. The as printed RD was determined to be 0.18.

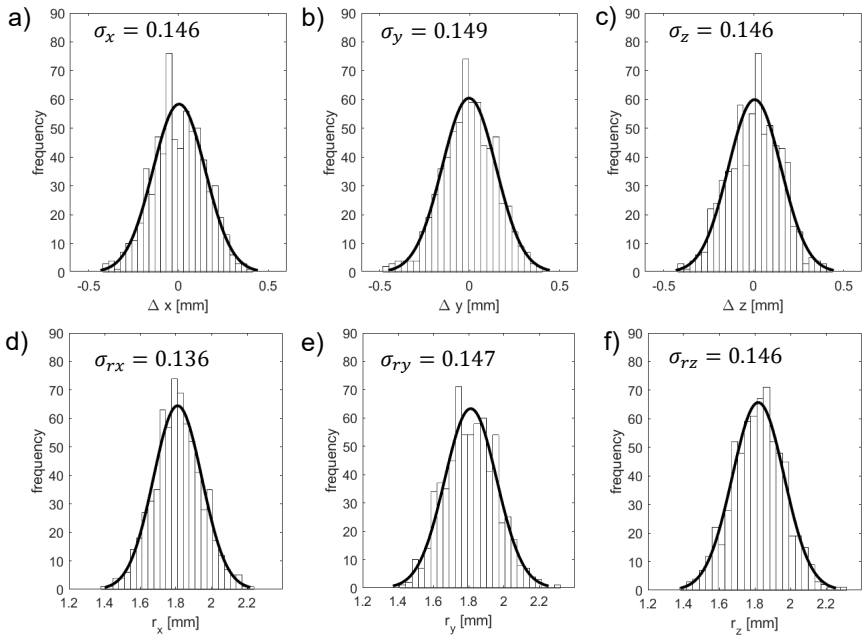

Figure 6: Evaluation of the ellipsoids' parameter-set of the isotropic FCC lattice. The input randomisation for all parameters is $\sigma = 0.15$, the RD is 0.2. a), b), c) show the added parameter $\Delta x, y, z$ to the x, y, z-coordinate and the corresponding standard deviation $\sigma_{x,y,z}$. d), e), f) show the randomised ellipsoids' radii and the their standard deviation $\sigma_{rx,ry,rz}$.

3.2. Function II: Anisotropic Randomness

Anisotropic randomness is shown in fig. 7, where every ellipsoid's parameter (eq. (1)) has a different randomisation value σ. a) - c) show the randomisation of the radii in the x, y, and z-direction. d) - f) show the randomisation of the centre position of each ellipsoid. An anisotropic lattice structure can be constructed by superimposing all six different randomisation possibilities as illustrated in g). In the bottom part of g), a SLS example of the anisotropic lattice is presented.

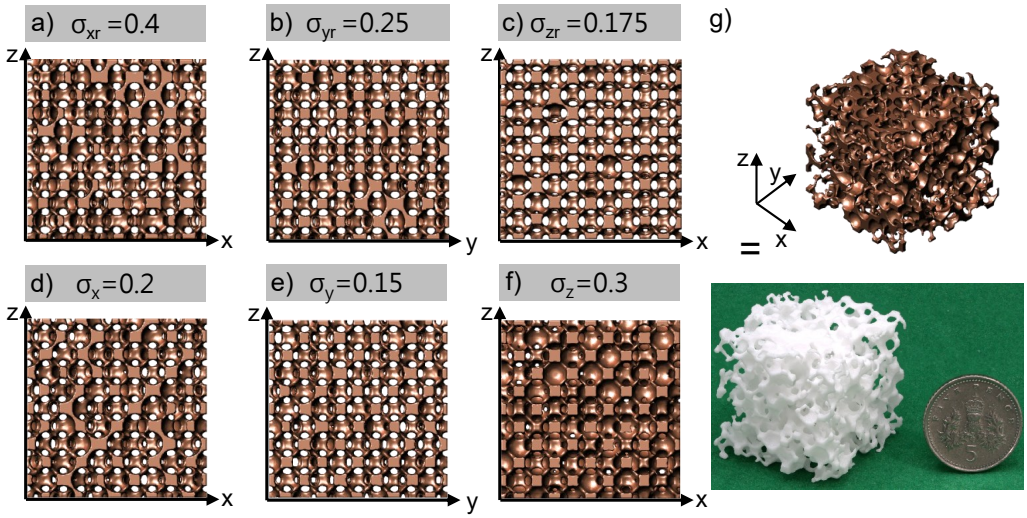

Figure 7: Six parameters of an FCC lattice were randomised by six different randomisation parameters. In a) to c), the ellipsoid's radii are randomised, while in d) to f), the ellipsoid's centre positions are randomised. Anisotropic randomness as illustrated in g) is achieved by superimposing all six demonstrated randomisation possibilities. Moreover, SLS was used to manufacture the anisotropic random lattice. The British five pence coin is 18 mm in diameter.

3.3. Function III: Graded Randomness

In fig. 8, four examples to grade randomness to an FCC lattice are shown. a) - c) show the principles of grading the ellipsoid's radius and center randomisation in x, y, and z-direction, respectively. In a) the lattice is graded from 0 to 0.3, in b) from 0 to 0.25 and c from 0 to 0.2. All three examples show how the initial regular structure gradually becomes more random. An anisotropic graded randomness lattice can be created by superimposing these three examples as shown by way of example in fig. 8 d). d) shows the regular structure in the lower-left corner, while the graded randomness is different in all directions. The four demonstrated graded randomness lattices were also manufactured by SLS to demonstrate manufacturability. The manufactured lattices are shown below a) - c) and on the right of d).

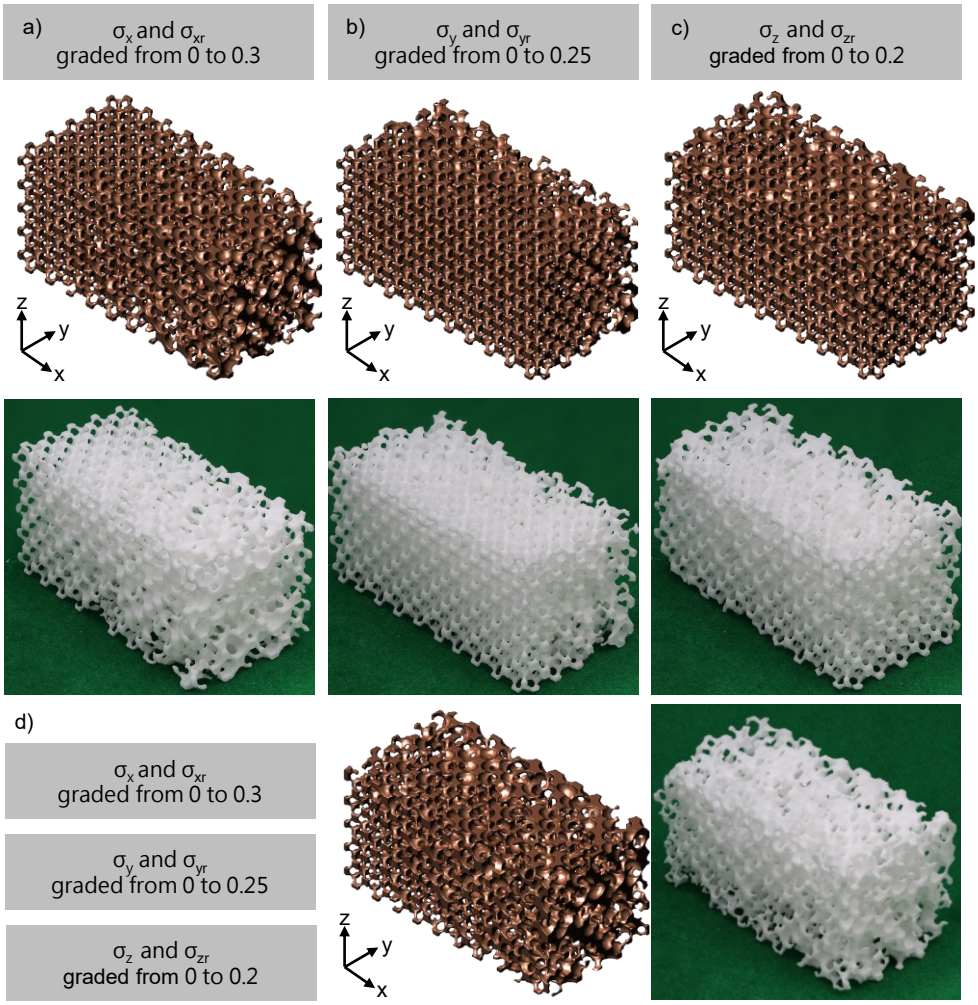

Figure 8: Graded randomness is demonstrated in three different directions with three different randomisation values in FCC lattices. a) the x-position and x-radius is randomised from 0 to 0.3, b) the y-position and the y-radius is randomised from 0 to 0.25, c) the z-position and the z-radius is randomised from 0 to 0.2. Superimposing the three different graded lattices a)-c) results in an anisotropic graded randomness lattice d). Lattices a)-d) were also manufactured via SLS.

3.4. Function IV: Layered Randomness

The method described in section 2.5 was used to create a layer with randomness in an FCC lattice cube, as illustrated in fig. 9. As demonstrated in fig. 9 a), a flat layer can be constructed via the function (10) if the amplitude a is set to zero,

which means the sine part of the function is not applied. However, by increasing the amplitude a and changing the periodicity p a sine layer is created (fig. 9 b). Through increasing the periodicity p (fig. 9 c), the sine layer can be compressed. Stochastic layer examples can be manufactured via SLS as shown.

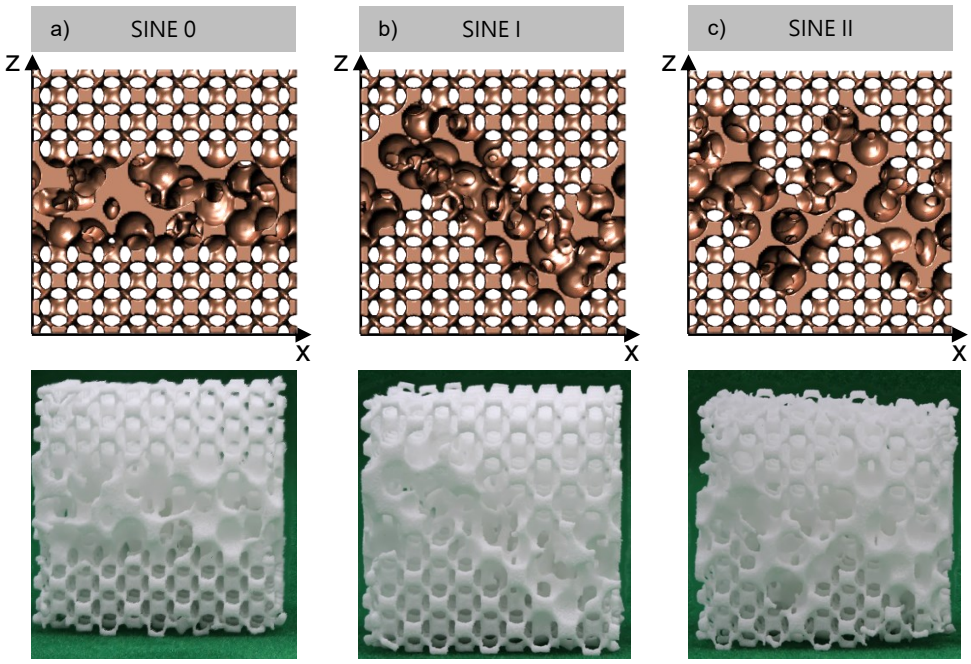

Figure 9: Three FCC lattices created with a stochastic layer by a sine function. a) is a layer within the FCC structure where the amplitude of the sine function is zero, resulting in a flat layer. b) By increasing the amplitude of the sine function, a sine function occurs within the lattice. c) By changing the periodicity, the sine function is compressed in comparison to b). a-c) were manufactured via SLS.

3.5. Function V: Surface Roughness

The fifth tool is stochastic surface roughness. In fig. 10, two FCC type lattices of the same size are demonstrated. a) shows the original lattices that includes no roughness. Therefore a smooth surface can be seen when magnified. Superimposing a roughness (μ_{rough} and σ_{rough} = 0.2) results in a rough surface lattice as demonstrated in image b). Through additive manufacturing a) and b), it can be seen that the surface roughness can also be replicated via additive manufacturing (see protrusion in fig. 10 b) lower image).

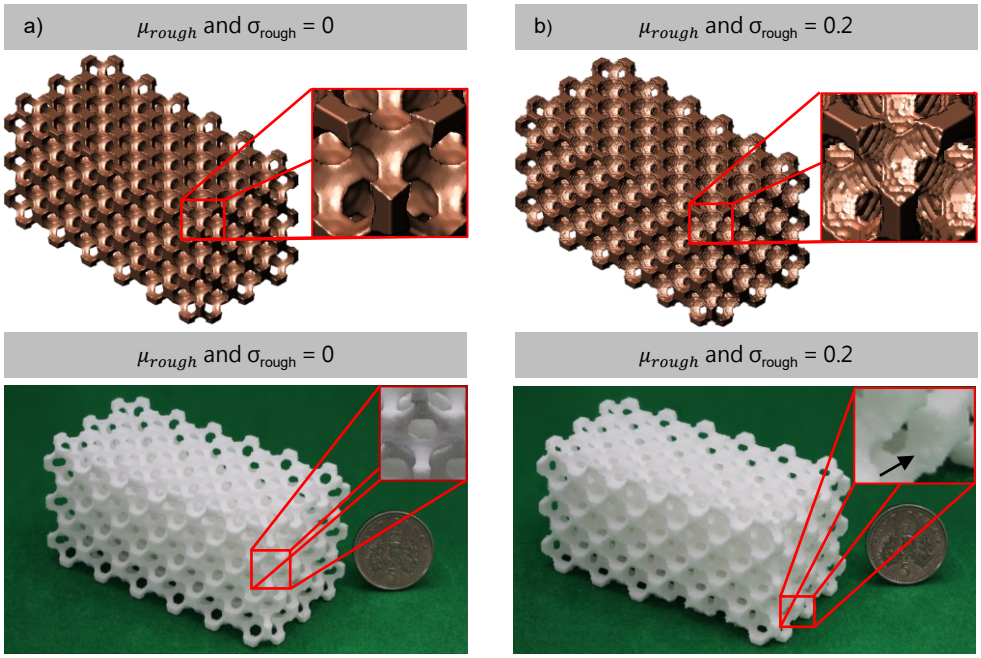

Figure 10: a) shows a smooth FCC lattice. roughness was applied to μ_{rough} and σ_{rough}. b) shows a lattice with superimposed roughness, where 0.2 was applied to both μ_{rough} and σ_{rough} . A SLS example of each lattice is presented. A British five pence coin (18 mm diameter) is shown for scale. The roughness in the SLS example in a) is shown and b) indicated by an arrow.

3.6. Stochastic Sculpture

In fig. 11, a hand is demonstrated that shows the lattices created by the five tools previously demonstrated (a hand geometry published on Thingiverse by George Weber [34] was used and lattices, logos and texts were added). All lattices are made from an FCC type lattice. The small finger represents the isotropic randomness; the ring finger is made from an anisotropic random lattice. The middle finger shows graded randomness, while the index finger includes a stochastic sine layer. The thumb represents the roughness layer. On the backside of the hand, a regular lattice is included and the fingers are stabilized through rods to prevent early failure. This design is intended as a demonstrator, therefore it includes the title of this paper and the authors' names and details of a forthcoming software package incorporating these methods. A demonstration was printed via SLS.

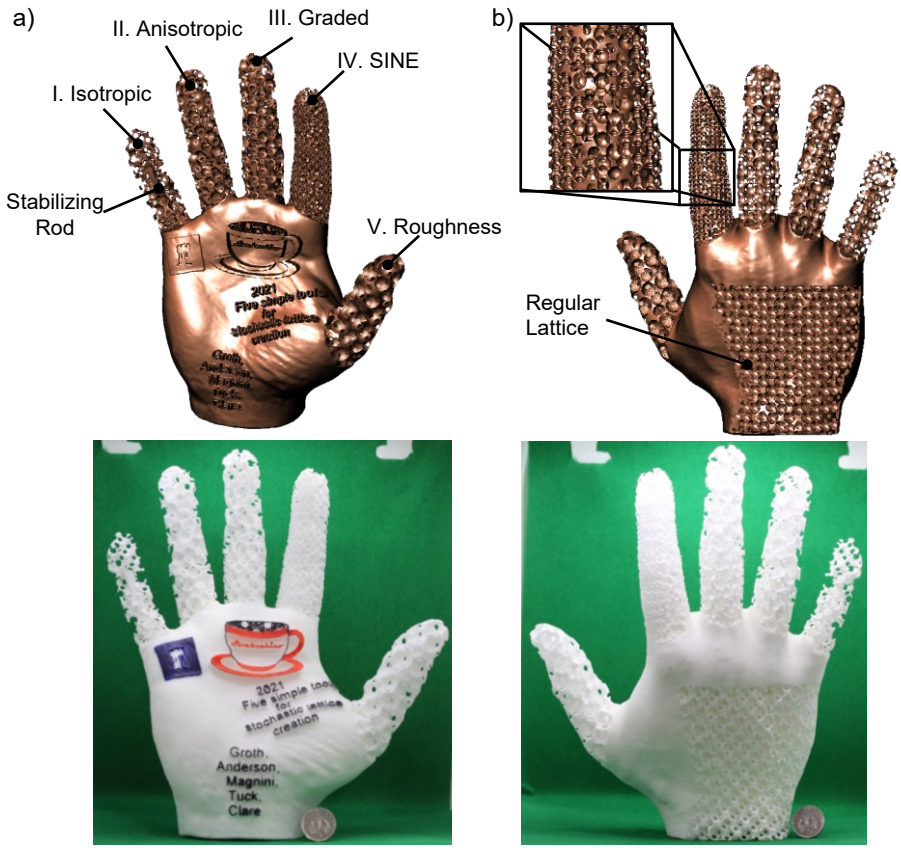

Figure 11: a) To illustrate the implementation of stochastic lattices the fingers of a hand show the five tools devised here. An FCC UC was used to illustrate each process. b) The sine layer within the index finger is highlighted. A regular FCC lattice is included on the backside of the hand. (The original hand geometry without lattices and text was published on Thingiverse by George Weber [34]) The British five pence coin is 18 mm wide.

4. Discussion

The purpose of this study was to expand the capability of stochastic design tools. We created regular location arrays on which we positioned spheres to create commonly known lattice types. We then superimposed various types of randomness on the sphere's location and manipulated the sphere's radii by assuming the sphere is an ellipsoid. This resulted in five simple tools to design stochastic lattices. Isotropic randomness is when the same randomness value is used for each parameter. Anisotropic randomness is when the randomness value is different for

each parameter. This should not be confused with the simple directional variation in properties of solid materials. Graded randomness is when the randomness value changes from a minimum value to a maximum value according to its location. A stochastic layer is a layer that is enclosed between two regular structures, has a specific thickness, location and can follow a defined function. A stochastic surface roughness is used to roughen the surface by a certain randomness value over the whole structure. The results are five tools that can be applied individually or in unison for many engineering applications.
The five tools can be compared and contrasted as follows to the most recent literature about the subject. The majority of stochastic designs are represented by strut based lattices of uniform thickness [20], but also stretched stochastic Voronoi lattices [18], [16], and the randomisation of implicit functions can be observed [10]. Here, we used ellipsoids that we extract from a solid, resulting in open and closed cells with varying strut thickness, which gives more randomisation possibilities than previously adopted lattice structures. The isotropic randomness tool is similar to techniques observable in older literature like [7] or newer literature like [20] or [18]. They applied the same randomness value for each parameter. This resulted in forming the idea to establish the manipulation of randomness itself. Furthermore, anisotropic randomisation can be distinguished from the isotropic randomness because for each parameter a different kind of randomness is used. Moreover, in the research field of lattices, it is common to grade the UC size or the relative density [23]. We transferred this to tailor randomness. Therefore we created a tool that changes the randomness linearly according to its location. This can easily be translated to nonlinear functions or localised around 'sensitiser' features. Different layers like sandwich structures are well understood, and in lattice designs, hybrid structures can be observed [35], where two different lattice structures morph into one another. However, we created a flat or sine shaped layer of randomness, which creates new application opportunities.

The demonstrated tools show the following limitations. Firstly, the mechanical or thermal properties are not known yet. Hence, the future research fields are speculative at this time. Secondly, the tools do not incorporate rules that could define relationships between the different randomness. For example, a rule could be to only allow the sizes of the ellipsoid to only permit a closed or open cell stochastic lattice to be created. Third, the stochastic surface roughness tool creates roughness but this needs to be linked to the specific additive manufacturing process to design surface roughness efficiently, for example for the purpose of increased heat transfer.
There are several fields where stochastic lattices could be applied. An application

for anisotropic randomness, graded randomness and stochastic surface roughness are medical engineering applications. Here, especially the design tools could aid the interaction between the bone structure and the lattice, and improve the already proposed design by Murr et al. [36], which shows differently sized random lattices. Moreover, studies confirm that random like lattices [37] increase the pull-out force of teeth implants and that circular pedestals randomly positioned on a surface improve osseointegration [38]. In mechanical engineering applications, these tools could be used to optimise frequency band gaps [39]. It could be assumed that the stochastic lattices compared to recently studied regular lattices [40] could help filter certain frequencies, especially when the acoustics might vary a lot. Furthermore, as recently shown, stochastic lattices absorb energy with distinct energy-time profiles [20]. This is compared to regular lattices where failure is a compound of discrete events where unit cells break in sequence. Hence these lattices could be used in energy absorption applications. Additionally, stochastic lattices could be used in thermo-mechanical applications, where the anisotropic and graded randomness could fulfil two functions. Wong et al. [41] could not show that lattices increase heat transfer because most of the lattice's struts were in the wake zone of the fluid and due to the lattice's channel like design the turbulence generation was poor. Stochastic lattices could overcome this problem because the struts would not be in line anymore. Moreover, due to this stochastic irregularity in the design, the boundary layer could be restrained from developing an unnecessary high thickness, thus resulting in higher heat transfer [42]. In summary the stochastic lattice is set to be an increasingly important design feature.

5. Conclusion

Here we demonstrated five tools to design a stochastic lattice, which were implemented in human a hand model, where each finger represents one design tool. Four lattices (Cubic, BCC, FCC, FCC+) can create a regular array of spheres on which we superimpose a Gaussian random distribution. This leads to a stochastic lattice. By tailoring the randomisation value, we achieve isotropic randomness, where the same randomness values are used throughout the system. Anisotropic randomness is achieved when we apply for each design parameter a different randomisation value. Graded randomness can be achieved by applying a linear function to the randomisation value and superimpose it on the regular lattice structure. By applying a sine function, we can create a flat or curved stochastic layer. By altering the surface of the solid with the explained stochastic function we can create stochastic surface roughness. To demonstrate the five tools' additive manufactura-

bility. All five tools were demonstrated by an additive manufactured SLS example. The results are five tools that can be applied in medical engineering, mechanical engineering and thermo-mechanical designs. This opens new opportunities for research in said fields.

Acknowledgements

We thank Mr Adam Whitbread for preparing files and manufacturing the lattices and hand shown in this work. Professor Clare would like to acknowledge the kind support of the Royal Academy of Engineering, RCSRF1920927.

References

[1] L. J. Gibson, M. F. Ashby, Cellular solids: Structure and properties (1997).

[2] M. Benedetti, A. Du Plessis, R. Ritchie, M. Dallago, S. Razavi, F. Berto, Architected cellular materials: A review on their mechanical properties towards fatigue-tolerant design and fabrication, Materials Science and Engineering: R: Reports 144 (2021) 100606.

[3] M. F. Ashby, T. Evans, N. A. Fleck, J. Hutchinson, H. Wadley, L. Gibson, Metal foams: a design guide, Elsevier, 2000.

[4] J. Tian, T. Kim, T. Lu, H. Hodson, D. Queheillalt, D. Sypeck, H. Wadley, The effects of topology upon fluid-flow and heat-transfer within cellular copper structures, International Journal of Heat and Mass Transfer 47 (14-16) (2004) 3171–3186.

[5] A. Seharing, A. H. Azman, S. Abdullah, A review on integration of lightweight gradient lattice structures in additive manufacturing parts, Advances in Mechanical Engineering 12 (6) (2020) 1687814020916951.

[6] O. Al-Ketan, R. K. Abu Al-Rub, Multifunctional mechanical metamaterials based on triply periodic minimal surface lattices, Advanced Engineering Materials 21 (10) (2019) 1900524.

[7] M. Van der Burg, V. Shulmeister, E. Van der Geissen, R. Marissen, On the linear elastic properties of regular and random open-cell foam models, Journal of Cellular Plastics 33 (1) (1997) 31–54.

[8] A. Roberts, E. J. Garboczi, Elastic properties of model random three-dimensional open-cell solids, Journal of the Mechanics and Physics of Solids 50 (1) (2002) 33–55.

[9] M. H. Luxner, J. Stampfl, H. E. Pettermann, Numerical simulations of 3d open cell structures–influence of structural irregularities on elasto-plasticity and deformation localization, International Journal of Solids and Structures 44 (9) (2007) 2990–3003.

[10] N. Yang, L. Gao, K. Zhou, Simple method to generate and fabricate stochastic porous scaffolds, Materials Science and Engineering: C 56 (2015) 444–450.

[11] M. J. Silva, W. C. Hayes, L. J. Gibson, The effects of non-periodic microstructure on the elastic properties of two-dimensional cellular solids, International Journal of Mechanical Sciences 37 (11) (1995) 1161–1177.

[12] H. Zhu, J. Hobdell, A. Windle, Effects of cell irregularity on the elastic properties of open-cell foams, Acta Materialia 48 (20) (2000) 4893–4900.

[13] H. Zhu, A. Windle, Effects of cell irregularity on the high strain compression of open-cell foams, Acta Materialia 50 (5) (2002) 1041–1052.

[14] H. Zhu, J. Hobdell, A. Windle, Effects of cell irregularity on the elastic properties of 2d voronoi honeycombs, Journal of the Mechanics and Physics of Solids 49 (4) (2001) 857–870.

[15] H. Zhu, S. Thorpe, A. Windle, The geometrical properties of irregular two-dimensional voronoi tessellations, Philosophical Magazine A 81 (12) (2001) 2765–2783.

[16] J. Martínez, J. Dumas, S. Lefebvre, Procedural voronoi foams for additive manufacturing, ACM Transactions on Graphics (TOG) 35 (4) (2016) 1–12.

[17] J. Martínez, H. Song, J. Dumas, S. Lefebvre, Orthotropic k-nearest foams for additive manufacturing, ACM Transactions on Graphics (TOG) 36 (4) (2017) 1–12.

[18] M. McConaha, S. Anand, Design of stochastic lattice structures for additive manufacturing, in: International Manufacturing Science and Engineering Conference, Vol. 84256, American Society of Mechanical Engineers, 2020, p. V001T01A036.

[19] M. Mirzaali, R. Hedayati, P. Vena, L. Vergani, M. Strano, A. Zadpoor, Rational design of soft mechanical metamaterials: Independent tailoring of elastic properties with randomness, Applied Physics Letters 111 (5) (2017) 051903.

[20] J. Mueller, K. H. Matlack, K. Shea, C. Daraio, Energy absorption properties of periodic and stochastic 3d lattice materials, Advanced Theory and Simulations 2 (10) (2019) 1900081.

[21] G. Maliaris, A. Argyros, E. Smyrnaios, N. Michailidis, Novel additively manufactured bio-inspired 3d structures for impact energy damping, CIRP Annals (2021).

[22] O. Al-Ketan, R. K. Abu Al-Rub, Mslattice: A free software for generating uniform and graded lattices based on triply periodic minimal surfaces, Material Design & Processing Communications (2020) e205.

[23] I. Maskery, A. Aremu, L. Parry, R. Wildman, C. Tuck, I. Ashcroft, Effective design and simulation of surface-based lattice structures featuring volume fraction and cell type grading, Materials & Design 155 (2018) 220–232.

[24] M. Shomper, Designing lattice structures for biologically-relevant medical implants, https://ntopology.com/blog/2019/07/25/designing-lattice-structures-for-medical-implants/, accessed: 2021-10-12 (2019).

[25] M. Shomper, Intentional design of surface roughness for orthopedic parts, https://ntopology.com/blog/2019/05/24/intentional-design-of-surface-roughness-for-orthopedic-parts/, accessed: 2021-10-12 (2019).

[26] Autodesk within medical, https://www.autodesk.com/products/within-medical/overview, accessed: 2021-10-18.

[27] L. Ventola, F. Robotti, M. Dialameh, F. Calignano, D. Manfredi, E. Chiavazzo, P. Asinari, Rough surfaces with enhanced heat transfer for electronics cooling by direct metal laser sintering, International Journal of Heat and Mass Transfer 75 (2014) 58–74.

[28] C. K. Stimpson, J. C. Snyder, K. A. Thole, D. Mongillo, Roughness effects on flow and heat transfer for additively manufactured channels, Journal of Turbomachinery 138 (5) (2016) 1–10.

[29] A. du Plessis, C. Broeckhoven, I. Yadroitsava, I. Yadroitsev, C. H. Hands, R. Kunju, D. Bhate, Beautiful and functional: a review of biomimetic design in additive manufacturing, Additive Manufacturing 27 (2019) 408–427.

[30] M. V. Ankhelyi, D. K. Wainwright, G. V. Lauder, Diversity of dermal denticle structure in sharks: Skin surface roughness and three-dimensional morphology, Journal of Morphology 279 (8) (2018) 1132–1154.

[31] I. C. Meier, C. Leuschner, Leaf size and leaf area index in fagus sylvatica forests: competing effects of precipitation, temperature, and nitrogen availability, Ecosystems 11 (5) (2008) 655–669.

[32] S. Holcombe, stlwrite - write ascii or binary stl files, `https://www.mathworks.com/matlabcentral/fileexchange/20922-stlwrite-write-ascii-or-binary-stl-files`, accessed: 2021-10-11 (2021).

[33] I. Maskery, I. Ashcroft, The deformation and elastic anisotropy of a new gyroid-based honeycomb made by laser sintering, Additive Manufacturing 36 (2020) 101548.

[34] G. Weber, Hand, `https://www.thingiverse.com/thing:1680395`, license: CC BY 4.0, accessed: 2021-09-07 (2016).

[35] D.-J. Yoo, K.-H. Kim, An advanced multi-morphology porous scaffold design method using volumetric distance field and beta growth function, International Journal of Precision Engineering and Manufacturing 16 (9) (2015) 2021–2032.

[36] L. E. Murr, Strategies for creating living, additively manufactured, open-cellular metal and alloy implants by promoting osseointegration, osteoinduction and vascularization: An overview, Journal of Materials Science & Technology 35 (2) (2019) 231–241.

[37] J. Z.-C. Chang, P.-I. Tsai, M. Y.-P. Kuo, J.-S. Sun, S.-Y. Chen, H.-H. Shen, Augmentation of dmls biomimetic dental implants with weight-bearing strut to balance of biologic and mechanical demands: From bench to animal, Materials 12 (1) (2019) 164.

[38] M. J. Dalby, N. Gadegaard, R. Tare, A. Andar, M. O. Riehle, P. Herzyk, C. D. Wilkinson, R. O. Oreffo, The control of human mesenchymal cell differentiation using nanoscale symmetry and disorder, Nature Materials 6 (12) (2007) 997–1003.

[39] M. Askari, D. A. Hutchins, P. J. Thomas, L. Astolfi, R. L. Watson, M. Abdi, M. Ricci, S. Laureti, L. Nie, S. Freear, et al., Additive manufacturing of metamaterials: A review, Additive Manufacturing (2020) 101562.

[40] W. Elmadih, D. Chronopoulos, J. Zhu, Metamaterials for simultaneous acoustic and elastic bandgaps, Scientific Reports 11 (1) (2021) 1–10.

[41] M. Wong, I. Owen, C. Sutcliffe, A. Puri, Convective heat transfer and pressure losses across novel heat sinks fabricated by selective laser melting, International Journal of Heat and Mass Transfer 52 (1-2) (2009) 281–288.

[42] R. K. Shah, D. P. Sekulic, Fundamentals of heat exchanger design, John Wiley & Sons, 2003.